Technische Universität Wien
Vienna University of Technology

Institute of Fluid Mechanics
and Heat Transfer
Vienna University of Technology
A-1040 Vienna, Austria

An experimental investigation of the double channel membrane pump

W. Zackl, H. Neth, H. Steinück[1]

1 Introduction

In this project a new valve-less pumping principle 'the double channel membrane pump' has been investigated. Up to now most of the investigations on valve-less pumping are concerned with physiology. Here a valve-less pumping principle has been introduced which has the potential to be used to in industrial applications like pumping suspensions with relatively large immersed particles or very fragile particles.

According to the ideas of W. Zackl test pumps have been constructed and measurements to determine the characteristics of the pump have been performed. Here we summarize the construction principle of the pump and the results of the measurements. The report is organized as follows: In section two 2 a brief description of the working principle is given. Then we introduce some dimensionless characteristic quantities which describe the performance of the pump. In section 4 we describe the test pumps and and section 5 describe the measurements and section 6 we present the results. Conclusions are drawn in section 7.

2 Working principle of the double channel membrane pump

The design principle of the pump is shown in figure 1: A channel with rigid walls is divided in its mid plane into two sub-channels. On the inflow side (left in figure 1) the sub-channels are separated by a rigid plate. At the trailing edge of the plate there is a flap which is moved periodically up and down. In the outflow section the sub-channels are separated by a membrane which is attached to the flap. Thus the motion of the flap will induce an excitation of the membrane. However, it is the interaction of the (periodically excited) membrane with the fluid in both channels which drives the flow through the pump. In figure 2 a different type of the pump is shown. Here the membrane is excited by a vertically reciprocating propulsion plate instead of a flap. The blurred trace of small particles indicate the motion of the fluid.

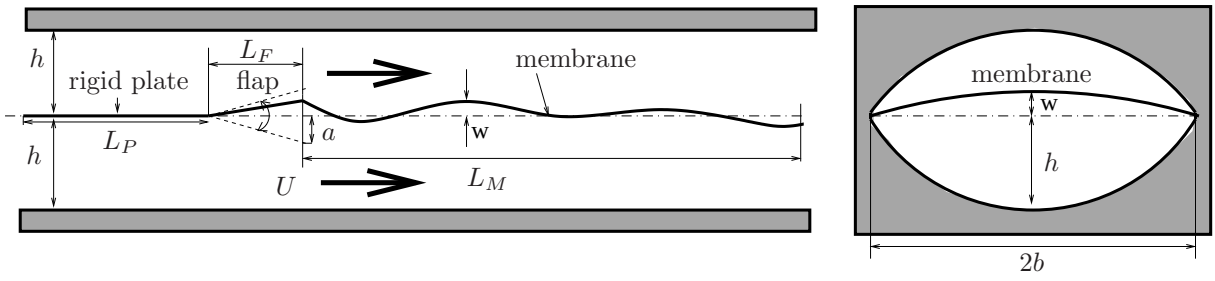

Figure 1: Sketch of double channel membrane pump

[1]E-mail herbert.steinrueck@tuwien.ac.at, address: Vienna University of Technology, Institute of Fluid Mechanics and Heat Transfer, Resselgasse 3, 1040 Vienna, Austria

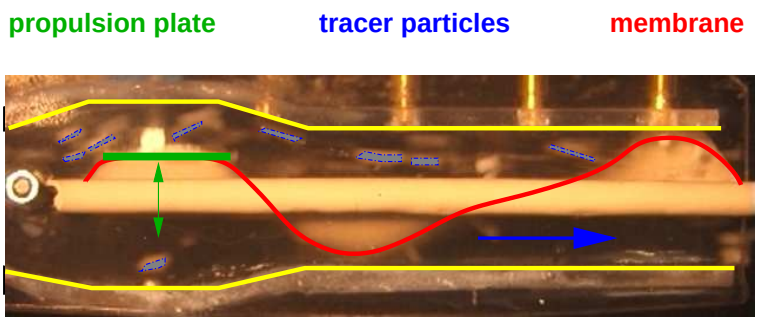

Figure 2: Demonstration model of double channel membrane pump. The membrane is excited by a vertically oscillating propulsion plate.

3 Dimensional Analysis

The first step of the analysis of the flow will be a dimensional analysis. Thus we refer all relevant quantities to suitable chosen reference values and identify dimensionless parameters. On one hand this reduces the number of parameters in the problem and on the other hand allows the comparison (or scaling) of flow configurations of different size.

In table 1 the most important parameters describing the double channel membrane pump and the operating conditions are listed.

L_F	length of flap	f	frequency
L_M	length of membrane	σ	stress of the membrane
L_P	length of plate	ν	kinematic viscosity
h	height of a half channel	$\bar{u}$	mean velocity
b	width of channel	p_{in}	pressure inlet
a	amplitude of flap motion	p_{out}	pressure outlet

Table 1: Parameters describing the flow through the membrane pump

We choose the length of the membrane as the basic length scale and refer all other lengths to it:

$$\delta_p = \frac{L_P}{L_M}, \quad \delta_f = \frac{L_F}{L_M}, \quad \delta_a = \frac{a}{L_M}, \quad \delta_h = \frac{h}{L_M}, \quad \delta_b = \frac{b}{L_M}.$$

To obtain a measure for the velocity fluctuation in longitudinal direction we consider the volume of fluid which is displaced when the flap moves from one extreme position to the other: $\Delta V = (a\, L_f)$. Thus the fluid of volume ΔV is shifted by the length of the order $L_D = \Delta V / A_{\text{cross}}$ in both channels, where A_{cross} is the cross section of one half-channel. Consequently a scale for the longitudinal velocity fluctuations u_F can be defined by

$$u_F = L_D\, f. \tag{1}$$

Having in mind the relation that the pressure difference across a membrane is of the order curvature of the membrane times the stress of of the membrane we introduce a parameter α describing the strength of the interaction of the fluid with the membrane. Let σ be the stress of the membrane in the non excited state and we estimate the curvature of the membrane by a/L_M^2 and use ρu_F^2 as a measure for the pressure difference between the two half-channels. Then we define the dimensionless stress parameter by

$$\alpha = \frac{\sigma}{\rho u_F^2} \frac{a}{L_M^2} = \frac{\sigma\, a}{\rho f^2 L_M^2 L_D^2}.$$

displaced volume	$\Delta V =$	$103\,\mathrm{cm}^3$
cross section of half channel	$A_{\mathrm{cross}} =$	$20,52\,\mathrm{cm}^2$
displacement length	$L_D = \Delta V / A_{\mathrm{cross}} =$	$10\,\mathrm{cm}$
membrane length	$L_M =$	$20\,\mathrm{cm}$

Table 2: Characteristic dimensions of the test pump

In the limit $\alpha \to 0$ the membrane does not influence the fluid at all, while the limit $\alpha \to \infty$ corresponds to a rigid separation of the two channels.

The parameter

$$\beta = \frac{p_{\mathrm{out}} - p_{\mathrm{in}}}{\rho f^2 L_D^2}$$

characterizes the pressure gain across the double channel membrane pump. The influence of viscosity in a pulsating flow is measured by the Womersley number

$$\mathrm{Wo} = \sqrt{\frac{h\, L_D f}{\nu}},$$

which can be interpreted as the square root of a Reynolds number based on the longitudinal fluctuation velocity u_F.

The Strouhal number

$$\mathrm{Sr} = \frac{L_D f}{\bar{u}} = \frac{u_F}{\bar{u}} =$$

is a reference value for the ratio of the mean flow velocity $\bar{u}$ and the velocity fluctuations u_F.

Using these definitions the Reynolds number based on the mean flow velocity $\bar{u}$ can be expressed as

$$\mathrm{Re} = \frac{\bar{u} h}{\nu} = \frac{\mathrm{Wo}^2}{\mathrm{Sr}}.$$

Thus the pump characteristics can be described in dimensionless form as

$$0 = F(\mathrm{Sr}, \mathrm{Wo}, \alpha, \beta, \delta_a, \delta_p, \delta_f, \delta_h, \delta_b, ...). \tag{2}$$

Consider the geometry and the membrane of a specific pump given then the parameters α, δ_a,..δ_b are fixed and equation (2) reduces to a relation between the Strouhal number Sr and the pressure gain factor β: $f(\mathrm{Sr}, \beta) = 0$ which can be interpreted as a dimensionless form of a so called Q, h (volume flow pressure height)-diagram.

If the membrane behaves nonlinear due to large deformations (large amplitudes) or non elastic material behave suitable additional non-dimensional parameters have to be defined.

Institute of Fluid Mechanics
and Heat Transfer
Vienna University of Technology
A-1040 Vienna, Austria

Figure 3: Drive and gearbox

4 Description of the test pump

4.1 The pump drive

The pump is mounted on a steel base plate, see figure 3. The electric motor is hinged on the base plate. Its position is fixed by a steel lever which is connected by a load cell to the base plate. Thus the driving torque of the motor can be measured. The driving torque is transmitted by a belt to a parallel axle. On this axle there is a heavy fly wheel on one end. At the other end of the axle which is in the gear box the tilt levers are mounted on eccentric tappets. On top of the gear box the holes for the bearings of the axle where the driving flap is mounted can be seen. To avoid vibrations a second set of tilting levers and flap axle is inserted on the lower sid of the gear box. In figure 3 the holes for the bearings of of the lower flap axle can be seen. The pump housing, see figure 4 will be mounted in the clearances on top of the gear box. The motor is a three phase asynchronous motor. Thus the speed can by controlled by the frequency of the applied a. c. current.

In figure 5 some of the small components of the pump can be seen: In the last row on the left there are two sets of tilting levers, one for the pumps and one for the dummy flap on the lower side of the gear box. The four glider bearings for the flap axles are made of bronze. One of them was later replace by a needle bearing. In the middle row the lateral cover plates with the slots for mounting the membrane can be seen. In the front row left there is the so called flap jaw. It is U-shaped with holes for the flap axles in its blades. The flap will be mounted onto the axle between the blades of the flap jaw. After that the membrane which consists of two layers will be clamped above and below the flap jaw. To avoid a cavity between the membrane and the flap the membrane will be fixed to the flap by small plates screwed onto of the flap figure 7

4.2 The membrane

4.2.1 design A

In figure 9 the cut of the blue print already copied to membrane is shown. On the left we see the part which will cover the flap jaw an the flap. The area where a small plate will clamp the membrane to the flap is indicated. A second layer of the membrane will be glued onto the dashed area. It should support the membrane in the region of highest loads. The parabolic form of the support layer of the membrane should somehow enhance the adjustment of the wave resistance at the trailing edge. The membrane will

Figure 4: Pump housing

Figure 5: Parts: Upper Row: 4 tilt levers, 2 cover plate, 4 bearings; Middle Row: lateral cover plate with slot to clamp the membrane and hole for axle, other distance and cover plates, front row: flap mouth with flap, axles, separator plates

date	series	material	thickness [mm]	design	strain	σ_x [N/mm]	σ_y [N/mm]	figure
01.09.06	I	A560 ShA 40	4	A	1.305	2.08	1.2	9
06.09.06	II	A560 ShA 40	2	A	1.379	1.24	0.74	10
19.09.06	III	Vulkollan ShA 80	2	A	1.226	9.00	5.0	11
26.09.06	IV	Vulkollan ShA 80	2	B	1.072	3.12	1.62	12

Table 3: Properties of test membranes

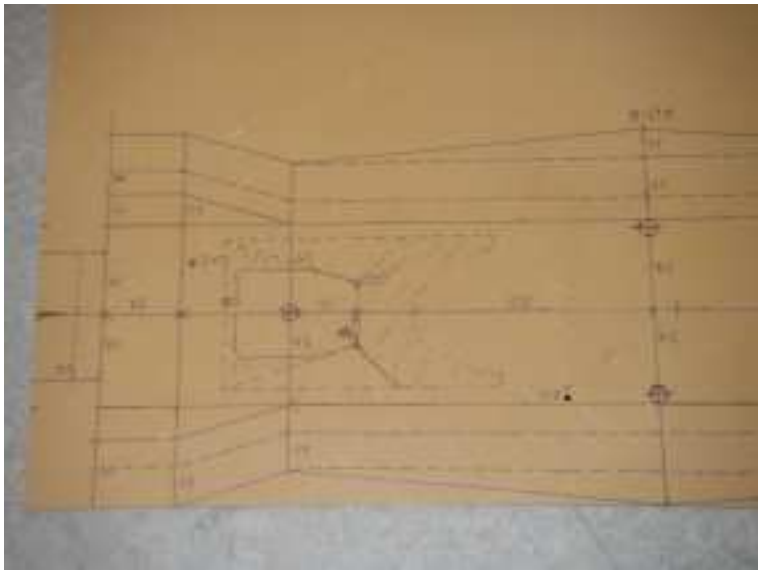

Figure 6: Cutting the membrane

be folded along the line on the right side of picture indicated as “Mitte”. Thus the membrane is double layered and fourth layered near the flap.

4.2.2 design B

In order two adjust the wave resistance better a second membrane design has been used. Near the trailing edge the membrane is reduced to a single layer. Thus a membrane of design B has four layers near the flap, then a two layer region follows and the final section consists of a single layer, see figure 12.

In order to measure the strain of the membrane a grid with mesh size 1 cm has been drawn on the undeformed membrane. Thus after mounting the membrane the length has been measured. and the stress has been calculated. To obtain the stress-strain relation tensile stress tests for the different material have been performed and the tension of the membrane in longitudinal σ_x and lateral σ_y tension is estimated using Rivilins[2] theory.

[2]R. S. Rivlin,Large elastic deformations of isotropic materials, I Fundamental concepts, Phil. Tran. A, **240**, pp 459-490, (1948).

Figure 7: Mounting the membrane

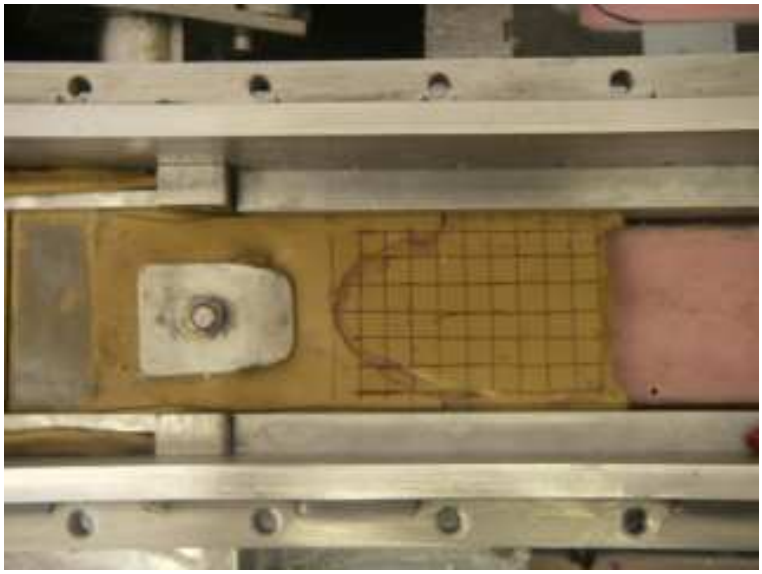

Figure 8: Membrane design A: unstrained

Figure 9: Membrane A560 ShA 40, 4 mm, design A, series I

Figure 10: Membrane A560 ShA 40, 2 mm, design A, series II

Figure 11: Membrane Vulkollan ShA 80, 2 mm, design A, series III

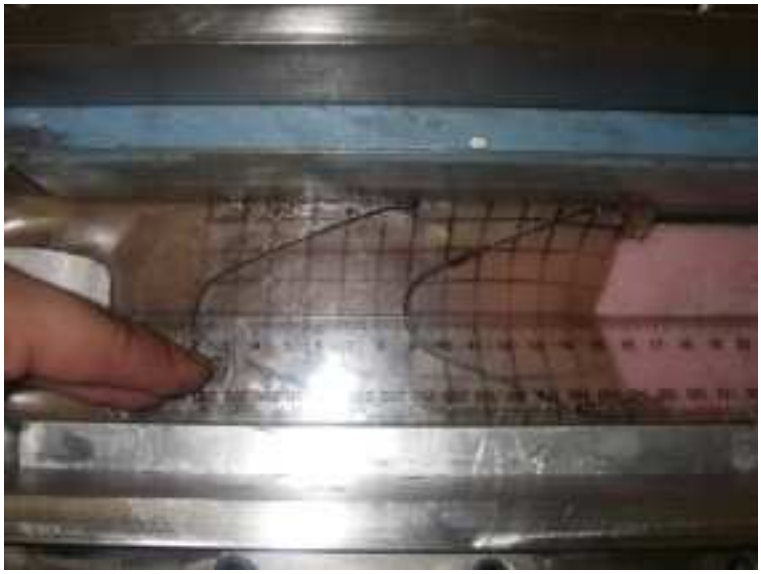

Figure 12: Membrane Vulkollan ShA 80, 2 mm, design B, series IV

Institute of Fluid Mechanics
and Heat Transfer
Vienna University of Technology
A-1040 Vienna, Austria

Figure 13: Double channel membrane pump and test section

5 Method of measurements

The double channel membrane pump has been integrated in a closed loop, see figure 13. A reservoir with a capacity of 0.5 m^3 is connected by a hose of diameter 6 cm to the inflow side of the pump. To stimulate a pressure increase after the pump a gate valve is inserted into the loop. From the gate valve the hose is directed back into the reservoir. In the reservoir a bucket of volume (51 dm^3) is inserted. Thus the flow rate can be determined by the filling time of the bucket, see figure 14.

Pressures are measured in the hoses before the pump and between the pump and the gate valve. Four sensors are used to record pressure signals: At the side walls before and after pump the (static) pressure is measured. The other two sensors are used to record the pressure in pitot tubes before and after the pump. From the difference between the pressures in the pitot tube and the pressures at the side walls the (instantaneous) flow rate can be determined. Of course this signal is highly oscillatory since the flow can be considered as a superposition of a uniform and a pulsating flow. For the evaluation of the flow rate the difference pressure has been averaged over a few periods of the flap oscillation.

The speed of the flap motion is controlled by the frequency of the a.c. current applied to the asynchronous motor which is generated by a frequency converter. Two modes of operation have been performed

- **static frequency STF**: the converter is switched to a constant frequency. Thus the flow rate can be determined by the volumetric flow measurement and from the difference of the static and dynamic pressure.
- **continuous frequency increase CFI**: The frequency converter can be programmed such that the frequency increases linearly with time at a rate of 0.8 Hz/s. Thus for this mode the flow rate can only be determined by the difference between the dynamic and static pressure as well.

In the plots of the measured results both the static and continuously increase frequency measurements are shown. Thus for the flow rate we have three curves: dynamic-static pressure difference measurement for the static and continuously increasing frequency operation mode and volumetric measurement for the static operation mode.

Figure 14: Volumetric measurement of flow rate

6 Results

In the tables 4-7 the results of the static (STF) measurements are listed. As discussed earlier for the flow rate the volumetric value and the value determined by the pitot tube are given. It turns out that the flow rate of the pitot tube is in general smaller than the volumetric one. If the gate valve is at position of 60° or higher the oscillations of the pressure signal are so high that no meaningful average can be defined.

In figures 15-18 the results of the STF and the CFI measurements are shown. Pressure-frequency, flow rate-frequency and flow rate-pressure diagrams are shown. Best results are obtained in case IV where pressures up to 0.51 bar are obtained. The Reynolds numbers are in the range of 1000 to 50000 such that in most cases we have a turbulent flow in the pump.

φ	f [Hz]	Δp [bar]	Q [m^3/h]	Q [m^3/h]	β	Sr	Re	Wo	α
0.00	8.83	0.01	9.30	7.96	3.57	1.64	5993.48	99.27	0.88
0.00	18.23	0.03	14.40	14.26	2.09	1.90	10734.16	142.67	0.21
0.00	27.10	0.04	15.70	19.26	1.15	2.09	14497.34	173.95	0.09
0.00	35.45	0.04	14.47	15.78	0.61	3.33	11881.76	198.95	0.05
20.00	8.83	0.02	7.86	7.36	5.67	1.78	5538.34	99.31	0.88
20.00	18.22	0.05	12.75	11.81	3.21	2.29	8890.18	142.64	0.21
20.00	27.09	0.07	14.18	14.56	2.01	2.76	10963.75	173.90	0.09
20.00	35.46	0.07	12.44	13.62	1.08	3.86	10255.71	198.99	0.05
40.00	8.89	0.04	4.52	4.41	10.71	2.99	3316.48	99.63	0.86
40.00	18.23	0.09	7.76	7.25	5.86	3.73	5457.36	142.69	0.21
40.00	27.09	0.15	9.99	9.38	4.33	4.29	7058.23	173.91	0.09
40.00	35.46	0.14	8.43	8.83	2.25	5.96	6648.43	198.99	0.05
60.00	8.87	0.06	1.41	1.62	15.39	8.14	1217.24	99.53	0.87
60.00	18.23	0.13	3.23	2.85	7.86	9.50	2142.42	142.66	0.21
60.00	27.10	0.23	5.53	4.16	6.42	9.66	3132.71	173.94	0.09
60.00	35.47	0.21	3.00	3.47	3.47	15.16	2612.23	199.00	0.05
70.00	8.92	0.07	0.75	0.77	16.93	17.15	580.40	99.78	0.86
70.00	18.26	0.14	1.98	1.18	8.45	22.94	888.56	142.78	0.20
70.00	27.12	0.25	4.00	1.52	6.88	26.43	1145.44	174.01	0.09
70.00	35.47	0.23	2.83	1.56	3.79	33.64	1177.23	199.00	0.05

Table 4: Series I: Static measurements

φ	f [Hz]	Δp [bar]	Q [m^3/h]	Q [m^3/h]	β	Sr	Re	Wo	α
0.00	8.83	0.01	9.30	7.96	3.57	1.64	5993.48	99.27	0.52
0.00	18.23	0.03	14.40	14.26	2.09	1.90	10734.16	142.67	0.12
0.00	27.10	0.04	15.70	19.26	1.15	2.09	14497.34	173.95	0.06
0.00	35.45	0.04	14.47	15.78	0.61	3.33	11881.76	198.95	0.03
20.00	8.83	0.02	7.86	7.36	5.67	1.78	5538.34	99.31	0.52
20.00	18.22	0.05	12.75	11.81	3.21	2.29	8890.18	142.64	0.12
20.00	27.09	0.07	14.18	14.56	2.01	2.76	10963.75	173.90	0.06
20.00	35.46	0.07	12.44	13.62	1.08	3.86	10255.71	198.99	0.03
40.00	8.89	0.04	4.52	4.41	10.71	2.99	3316.48	99.63	0.52
40.00	18.23	0.09	7.76	7.25	5.86	3.73	5457.36	142.69	0.12
40.00	27.09	0.15	9.99	9.38	4.33	4.29	7058.23	173.91	0.06
40.00	35.46	0.14	8.43	8.83	2.25	5.96	6648.43	198.99	0.03
60.00	8.87	0.06	1.41	1.62	15.39	8.14	1217.24	99.53	0.52
60.00	18.23	0.13	3.23	2.85	7.86	9.50	2142.42	142.66	0.12
60.00	27.10	0.23	5.53	4.16	6.42	9.66	3132.71	173.94	0.06
60.00	35.47	0.21	3.00	3.47	3.47	15.16	2612.23	199.00	0.03
70.00	8.92	0.07	0.75	0.77	16.93	17.15	580.40	99.78	0.51
70.00	18.26	0.14	1.98	1.18	8.45	22.94	888.56	142.78	0.12
70.00	27.12	0.25	4.00	1.52	6.88	26.43	1145.44	174.01	0.06
70.00	35.47	0.23	2.83	1.56	3.79	33.64	1177.23	199.00	0.03

Table 5: Series II: Static measurements

φ	f [Hz]	Δp [bar]	Q [m^3/h]	Q [m^3/h]	β	Sr	Re	Wo	α
0.00	8.84	0.01	6.95	5.73	2.12	2.29	4313.	99.36	3.78
0.00	17.96	0.04	16.83	16.61	2.56	1.60	12503.	141.61	0.92
0.00	26.67	0.06	19.66	19.85	1.62	1.99	14942.	172.56	0.42
0.00	35.30	0.05	18.77	18.53	0.90	2.83	13949.	198.54	0.24
20.00	8.88	0.01	6.49	5.32	3.72	2.48	4004.	99.59	3.75
20.00	17.96	0.07	14.61	13.00	4.27	2.05	9786.	141.61	0.92
20.00	26.66	0.10	17.67	17.87	2.81	2.21	13452.	172.54	0.42
20.00	35.30	0.09	17.08	17.54	1.56	2.98	13203.	198.53	0.24
40.00	8.90	0.03	4.32	3.77	7.71	3.50	2838.	99.71	3.73
40.00	17.98	0.13	9.16	8.34	8.15	3.20	6278.	141.71	0.91
40.00	26.66	0.20	11.77	10.52	5.75	3.76	7919.	172.53	0.42
40.00	35.30	0.22	12.37	11.85	3.66	4.42	8920.	198.54	0.24
60.00	8.94	0.05	1.93	1.57	12.75	8.45	1181.	99.93	3.70
60.00	18.01	0.17	3.74	3.44	10.72	7.76	2589.	141.80	0.91
60.00	26.64	0.29	5.40	4.32	8.30	9.15	3252.	172.48	0.42
60.00	35.31	0.35	5.25	4.46	5.68	11.74	3357.	198.56	0.24
70.00	8.95	0.06	1.19	0.67	14.61	19.81	504.	99.96	3.69
70.00	18.02	0.18	2.44	1.36	11.63	19.65	1023.	141.84	0.91
70.00	26.65	0.31	2.99	1.93	9.03	20.48	1452.	172.51	0.42
70.00	35.32	0.38	2.95	1.98	6.33	26.46	1490.	198.59	0.24

Table 6: Series III: Static measurements

φ	f [Hz]	Δp [bar]	Q [m^3/h]	Q [m^3/h]	β	Sr	Re	Wo	α
0.00	8.81	0.01	8.05	6.91	2.73	1.89	5201.75	99.20	1.34
0.00	17.95	0.05	18.77	17.48	3.34	1.52	13158.69	141.57	0.32
0.00	26.52	0.08	23.16	21.07	2.38	1.87	15861.19	172.09	0.15
0.00	35.08	0.09	23.17	23.97	1.44	2.17	18044.26	197.90	0.08
20.00	8.83	0.02	7.11	5.84	4.61	2.24	4396.27	99.31	1.34
20.00	17.96	0.09	15.62	14.58	5.43	1.83	10975.61	141.61	0.32
20.00	26.53	0.14	20.25	18.78	4.08	2.09	14137.31	172.09	0.15
20.00	35.10	0.16	20.20	19.99	2.65	2.60	15048.18	197.97	0.08
40.00	8.85	0.04	4.07	3.98	9.66	3.30	2996.09	99.39	1.33
40.00	17.97	0.14	10.01	9.15	8.78	2.91	6887.99	141.65	0.32
40.00	26.52	0.26	12.34	13.18	7.51	2.98	9921.71	172.09	0.15
40.00	35.09	0.32	13.98	14.36	5.38	3.62	10810.00	197.93	0.08
60.00	8.89	0.06	0.94	1.56	14.45	8.45	1174.35	99.61	1.32
60.00	17.99	0.18	3.25	3.40	11.56	7.85	2559.47	141.74	0.32
60.00	26.50	0.36	4.06	5.07	10.54	7.75	3816.62	172.01	0.15
60.00	35.10	0.46	5.88	5.27	7.63	9.88	3967.18	197.97	0.08
70.00	8.95	0.06	0.31	0.63	16.21	21.06	474.25	99.94	1.30
70.00	18.00	0.20	0.81	1.32	12.45	20.23	993.68	141.77	0.32
70.00	26.51	0.40	0.01	2.12	11.65	18.55	1595.90	172.04	0.15
70.00	35.08	0.51	1.91	2.06	8.45	25.26	1550.74	197.91	0.08

Table 7: Series IV: Static measurements

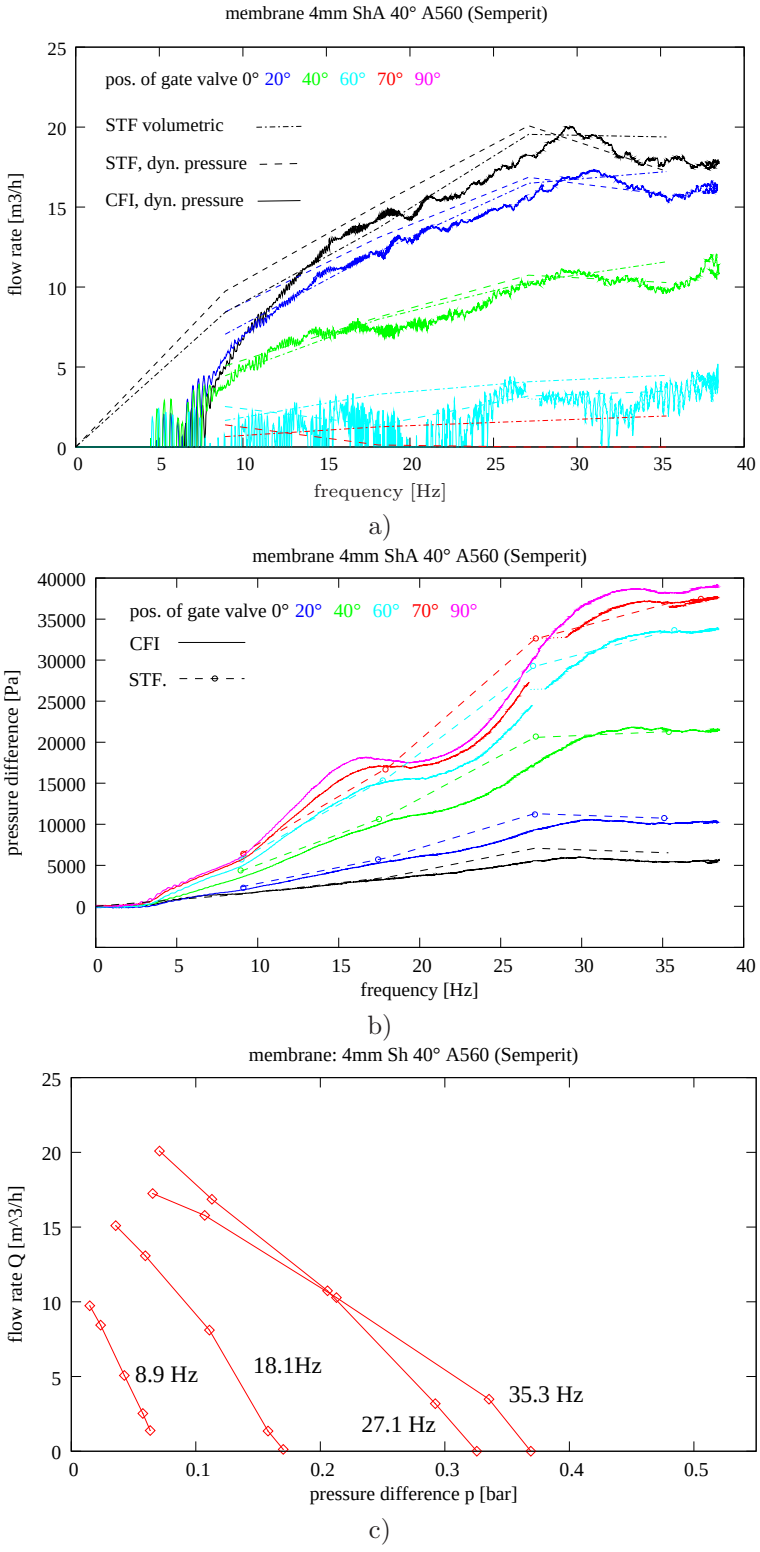

Figure 15: Case I: membrane 4 mm ShA 40, A560 (Semperit) a) flow rate, b) pressure difference b) as functions of the propulsion frequency, c) flow rate pressure diagram

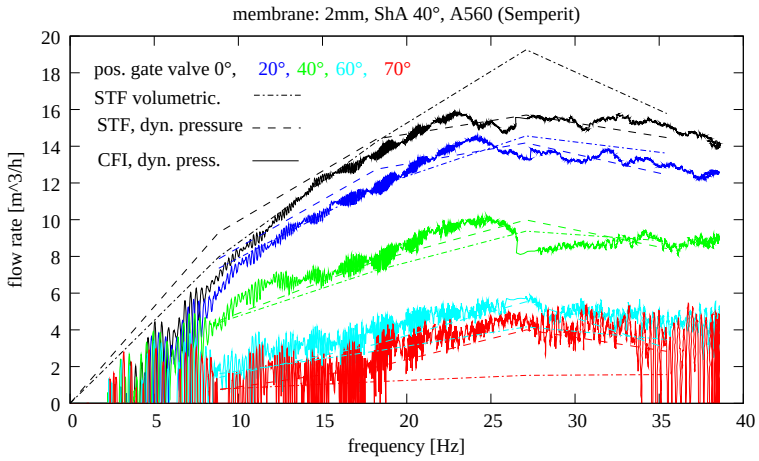

a)

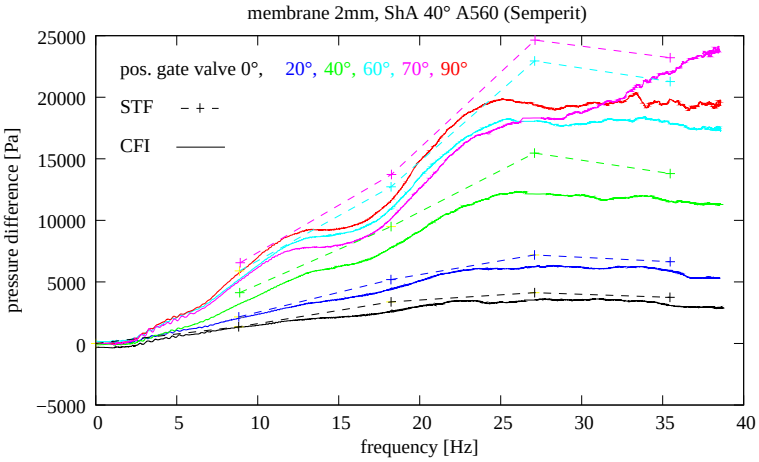

b)

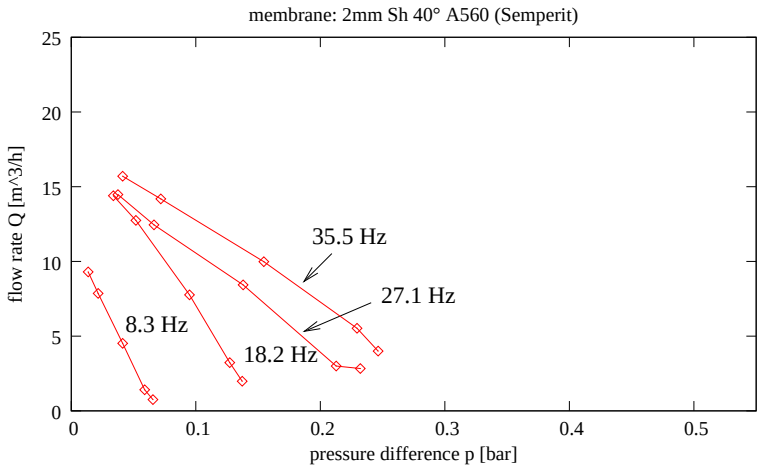

c)

Figure 16: CaseII: membrane 2 mm ShA 40 A560 (Semperit),a) flow rate, b) pressure difference b) as functions of the propulsion frequency, c) flow rate pressure diagram

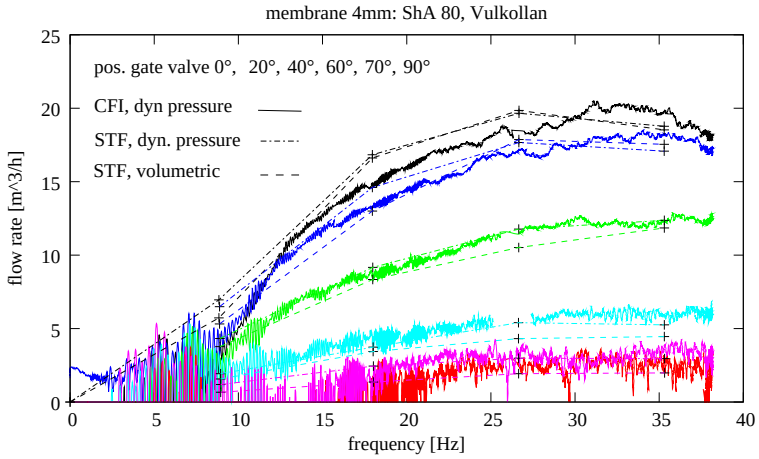

a)

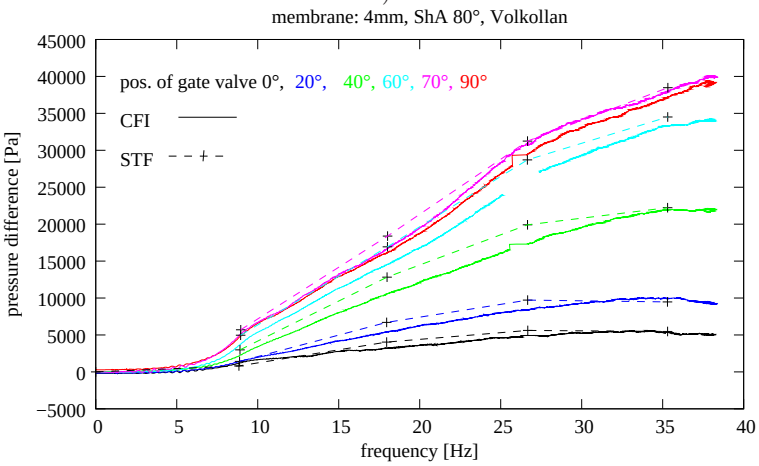

b)

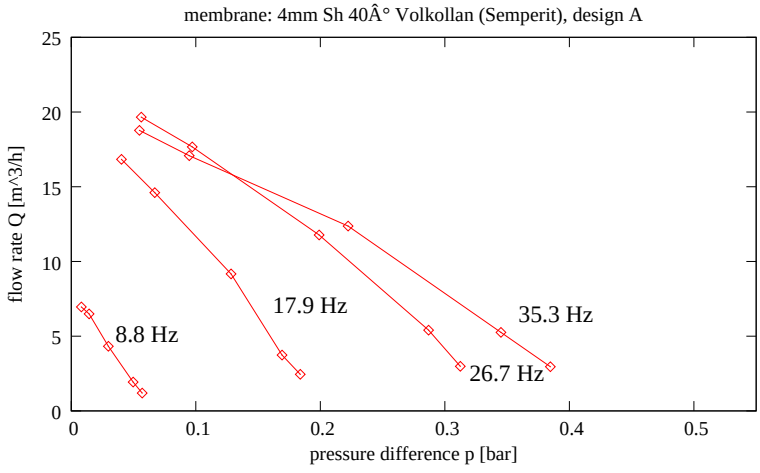

c)

Figure 17: Case III: membrane 4 mm ShA 80 Vulkollan Design A a) flow rate, b) pressure difference b) as functions of the propulsion frequency, c) flow rate pressure diagram

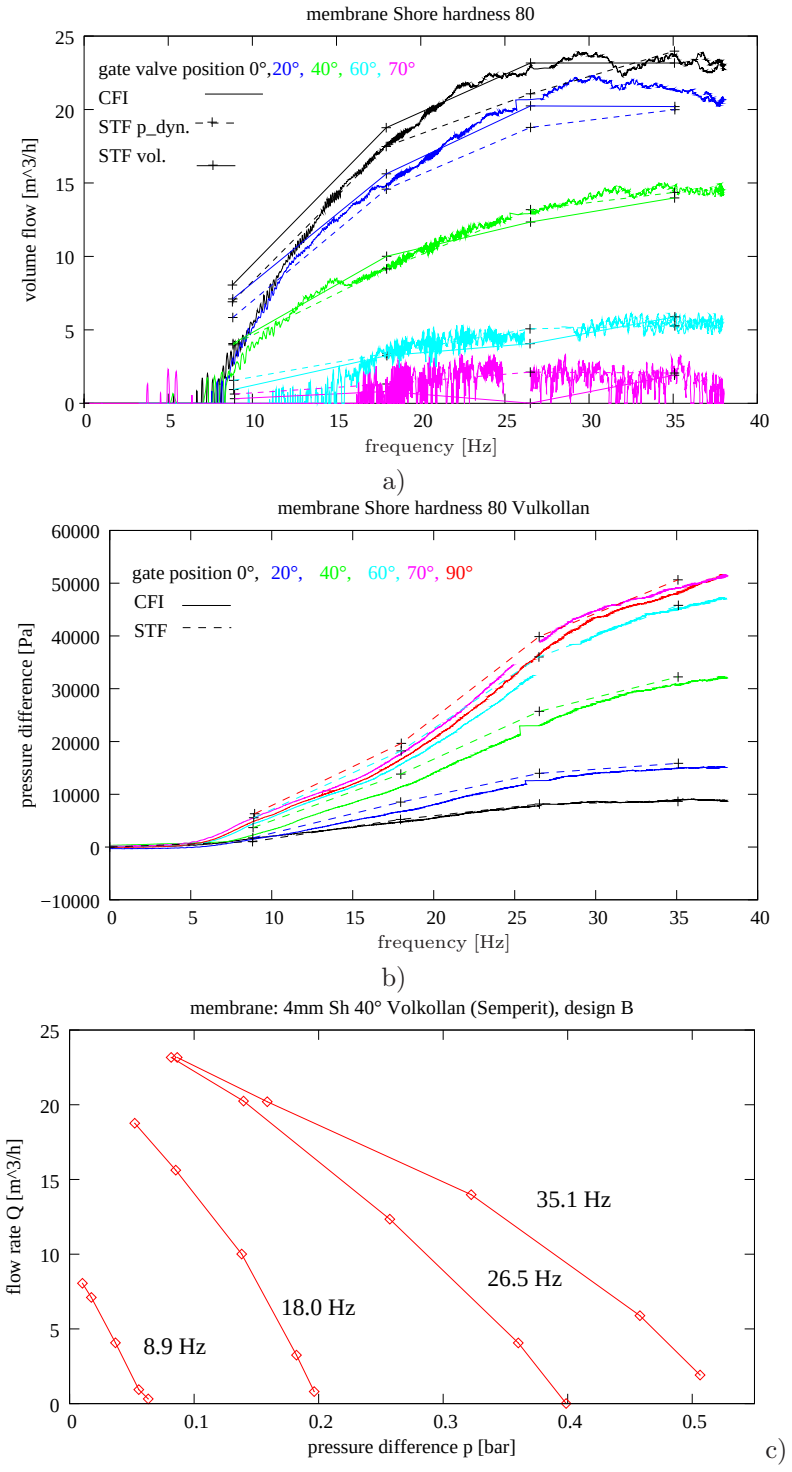

Figure 18: Case IV: membrane 4 mm ShA 80, Vulkollan, Design B a) flow rate, b) pressure difference b) as functions of the propulsion frequency, c) flow rate pressure diagram

position of gate valve	β	Sr
20°	3.6	2
40°	9.4	3
70°	14.4	20

Table 8: Empirical parameters for low frequency approximation for data from IV

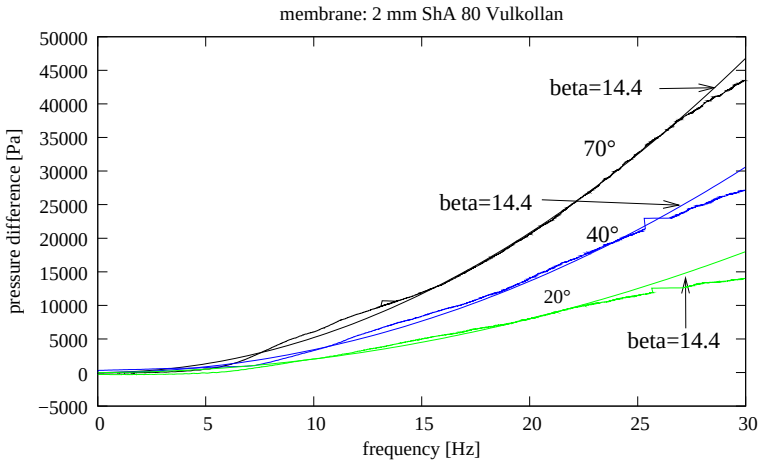

Figure 19: Comparisons measured results (CFI) with curves $\beta = \text{const}$.

6.1 Scaling laws

6.1.1 Low frequency approximation

From the measurements (flow rate 10 m^3/h, cross section 10 cm^2, height 1.7 cm, kinematic viscosity 10^{-6} m^2/s) the Reynolds number is estimated to be of the order of 40000. Thus we expect that the flow is almost inviscid and that the Reynolds number (or Womersley number) does not play a significant role. Assuming further that for weakly strained membranes and low frequencies the tension in the rest state has not much influence we conclude that β is a function of the Strouhal number and the geometrical parameters only.

$$\beta = f(\mathrm{Sr}, \delta_a, \delta_b, ...).$$

Inspecting the data for the case with the membrane design B we observe that the Strouhal number is almost constant for frequencies below 25 Hz. Thus we can approximate the pressure frequency curve in that range by a parabola. the pressure frequency curves for the measurements of series IV (membrane design B) with β constant.

In figure 19 curves $\beta = \text{const}$ are compared with the date from measurement series IV (CFI). For frequencies below 25 Hz the agreement we observe a good agreement.

series	f_s [Hz]	p_s [bar]	Q_s [m^3/h]
I.	52.6	0.178	2.0
II	40.0	0.100	1.0
III	88.9	0.333	1.1
IV	100.0	0.500	1.8

Table 9: Empirical scaling law: reference values

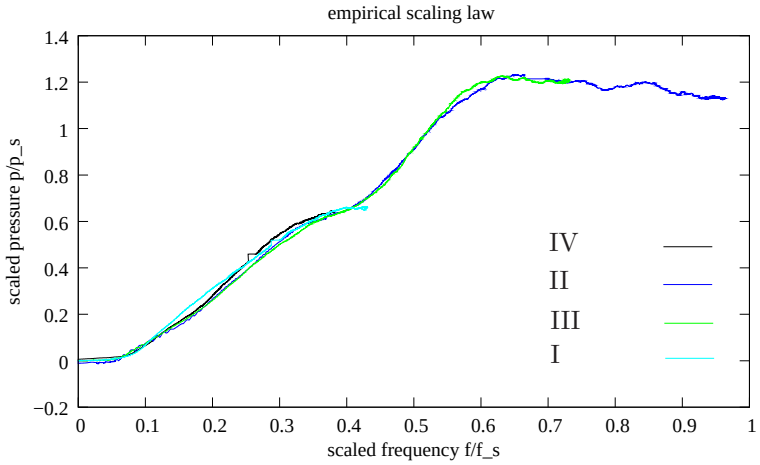

Figure 20: Empirical scaling law, gate valve: 40°

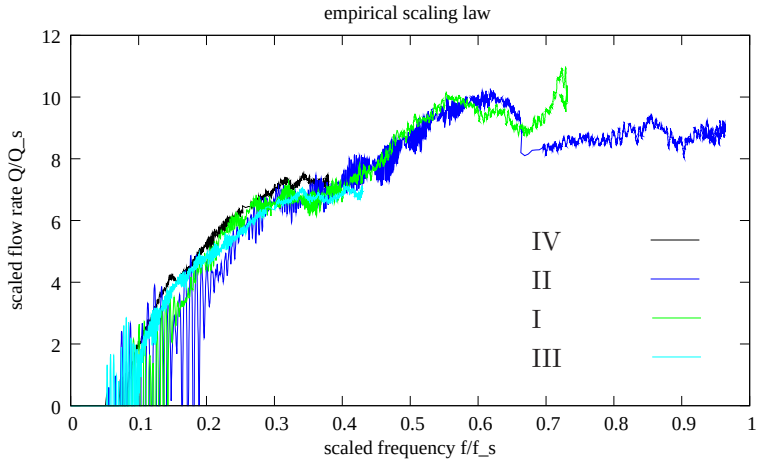

Figure 21: Empirical scaling law, gate valve: 40°

6.1.2 Empirical master curve

Comparing the results of measurements with continuously increasing frequency for the four different membranes at a gate valve opening of 40° we observe that the pressure frequency and the flow rate - frequency curves can be mapped to unique master curves when scaling the results appropriately. In table 9 the empirically determined scaling values for the pressure and flow rate are listed. In the figures 20, 21 the scaled curves are shown. The scaled pressure frequency curves are almost identical. The flow-rate frequency curves agree also astonishingly well. However, due to the large pressure variations when using the membranes made of A560 the flow rate signal is oscillatory. At the moment we have no theoretical explanation for this surprising scaling behavior.

7 Conclusions

- It has been shown that the double channel membrane pumping principle can be applied to technical relevant operating conditions.
- Different types of membranes have been tested. It has been observed that the efficiency increases if the tension of the membrane is increased. The results of the series IV seem to contradict this observation at first glance. But having in mind that the membrane is elongated up to 20% by the excitation of the flap the initially low stress (3.2 N/mm) will rise to about (9 N/mm) which of the same order as the stress in case III.

  An increase of stress can been achieved by three different methods:

  - increase of strain:
  - increase of thickness
  - increase of hardness

  It turned out that the increase of hardness gives the best results. Increase of the frequency results in general in higher pressures and flow rates. However, the tests with A560 showed that after an initial pressure increase with increasing the frequency a plateau is reached and a further increase of the frequency does not increase the pressure or the flow rate. During tests with Vulkollan the plateau has not been reached. We expect that with increasing frequency the flow rate and the pressure gain will increase further and eventually a plateau will be reached. Due to technical restrictions (glider bearings) the frequency has been limited to 40 Hz.
- Shape of the membrane: Most interestingly the design of the membrane has a remarkable influence on the performance of the pump. We interpret this phenomenon that in case of membrane design B the reflected waves are (at least partially) suppressed. The design B has been obtained by trying to adjust the wave resistance smoothly to zero at the trailing edge to prevent reflections.
- Vulkollan with Shore hardness 80 turned out to be the ideal membrane material.
- An empirical scaling law has been observed such that the pressure-frequency and flow rate-frequency curves can be mapped to universal master curves depending only on the opening of the gate valve.
- An estimate on efficiency in terms of resulting the hydraulic work $Q\Delta p$ to the mechanical (or electrical) power input could not be performed. It turned out by torque measurements in idle operation (with out a membrane and water) that the losses in the glider bearings are too high to make meaningful estimates. Thus the glider bearings have to be changed to needle bearings and all loses of the drive have to be checked before a decisive statement can be made.

7.1 Further investigations

- At the institute a theoretical analysis with a CFD program (FLUENT) is planned. The interaction of the almost massless membrane with the incompressible flow fields is a computational challenge where new efficient methods have to be developed.
- Experimentally we propose further investigations with different membranes and channel designs in order to get a better adjustment of the wave resistance at the trailing edge of the membrane. We are sure that substantial improvements can be made.
- Measurements of the overall efficiency should be performed. Thus the drive has to be improved to minimize mechanical losses. (Needle bearings instead of glider bearings).
- A further increase of the pressure can be obtained by increasing the displaced volume during a stroke by increasing the length of the flap.
- Experiments to determine the internal flow using PIV (particle image velocimetry) are desirable. To that purpose a transparent pump has to be build.
- The durability of the membrane should be tested. During the tests with the membrane of design B no signs of wear have been observed. But the operating time has been too short to make reliable statements.